DOI: https://doi.org/10.62985/j.huit_ojs.vol26.no2E.397

ELECTROMAGNETIC VIBRATION ANALYSIS OF POWER TRANSFORMER WINDINGS: VERIFICATION OF STRUCTURAL MODELS BASED ON ANALYTICAL MODELING

Khanh Le-Tran[1], Cuong Bui-Cong[1], Tu Nguyen-Ngoc[1], Nghia Pham-Dai[2], Huan Pham-Duy[3], Tuan Phung-Anh[1]*

[1]*Department of Electrical Engineering, Hanoi University of Science and Technology, Vietnam*

[2]*Advisory Board Member, EVN Hanoi Power Corporation, Vietnam*

[3]*Technical Department Head, EVN Hanoi Power Corporation, Vietnam*

*Email: *tuan.phunganh1@hust.edu.vn*

Received: 16 December 2025; Revised: 22 March 2026; Accepted: 28 April 2026

ABSTRACT

Excessive vibration in power transformers is a critical issue that compromises mechanical integrity, may result in insulation failure, and generates significant acoustic noise. Consequently, establishing a reliable method to quantify and predict these vibrations during the design phase is essential. This paper proposes a rigorous multiphysics simulation framework to analyze the vibration characteristics of a 40 MVA transformer winding. To validate the accuracy of the numerical approach, the study employs a systematic verification process based on analytical modeling. Initially, a fundamental beam model is utilized as a benchmark. The natural frequencies calculated via analytical solutions are compared with simulation results to confirm the correctness of mesh settings and boundary conditions. This agreement supports the assumption that the winding material behaves within the linear elastic region under harmonic excitations. Subsequently, the electromagnetic force distribution acting on the winding is computed using Finite Element Analysis. These forces are then applied to the verified structural model to determine the winding's natural frequencies and forced vibration response. The results demonstrate that verifying numerical models against analytical theory provides a robust foundation for assessing transformer vibration risks.

Keywords: Power transformer, electromagnetic vibration, multiphysics simulation, analytical verification.

1. INTRODUCTION

Power transformers are critical components in electrical grids. In rapidly urbanizing countries, substations are increasingly located in densely populated areas, making transformer noise and vibration a significant environmental concern [1], [2]. Transformer vibration primarily originates from two sources: magnetostriction in the magnetic core [3], [4], [5], [6]and electromagnetic forces in the windings [7], [8]]. While magnetostriction is a major source of acoustic noise, excessive winding vibration is often more detrimental to long-term structural integrity. Under the continuous action of electromagnetic forces, persistent vibration induces mechanical fatigue in clamping structures and more critically, causes irreversible abrasion of the paper insulation. This gradual degradation can be difficult to detect in early stages and may eventually lead to inter-turn short circuits, resulting in operational failures and potential power outages [9], [10]. Therefore, developing a reliable method to predict winding vibration is essential for both noise mitigation and operational safety.

To analyze these vibrations, engineers traditionally relied on simplified analytical formulas [1]. But these methods struggle with the complex geometries of modern transformers. Moreover, contemporary transformer design faces a stringent trade-off between mechanical robustness and material efficiency. To reduce material costs and improve cooling performance, modern designs tend toward increased compactness and reduced mass. This optimization lowers the structural stiffness of the windings and shifts their natural frequencies, thereby increasing their susceptibility to resonance with the 100 Hz electromagnetic excitation. With advances in computational capabilities, Finite Element Analysis (FEA) has evolved into the industry standard for multiphysics simulation, enabling high-fidelity coupling of electromagnetic and structural domains [11]-[13].

Despite its popularity, FEA entails a risk of "black box" uncertainty where incorrect inputs, such as mesh settings or boundary conditions, can lead to misleading results. Furthermore, the design process lacks a systematic approach to validate complex numerical models against fundamental analytical models. This is a critical issue for medium-power transformers, where experimental testing is often limited. Unvalidated models risk either over-design or undetected resonance phenomena.

This paper addresses this gap by proposing a simulation framework for a 40 MVA transformer winding. The study makes two key contributions. First, it establishes a verification strategy using a fundamental beam model by validating the natural frequencies against analytical solutions. This process demonstrates the physical fidelity of the numerical model and effectively mitigates the “black box” uncertainty inherent in FEA. Second, this validated framework is applies to analyzing the forced vibration response of a 40 MVA power transformer under rated load conditions, revealing a proximity between the winding's natural frequency and the excitation source. This finding provides quantitative evidence of resonance risks that are often overlooked in conventional static design.

2. THEORETICAL MODEL FOR TRANSFORMER WINDINGS VIBRATION

2.1. Electromagnetic Equations

The vibration of the transformer windings is fundamentally driven by the interaction between the time-varying current and the leakage magnetic field. In the transient finite element analysis, the magnetic field distribution is governed by Maxwell's equations using the magnetic vector potential *(A)* formulation [1]. For the winding modeled as stranded conductors (to suppress skin and proximity effects), the current density is dominated by the source excitation. Thus, the governing equation is expressed as:

$$\boldsymbol{\nabla} \times \left(\frac{\mathbf{1}}{\boldsymbol{\mu}}\boldsymbol{\nabla} \times \boldsymbol{A}\right) = \boldsymbol{J_e(t)} - \boldsymbol{\sigma}\frac{\boldsymbol{\partial A}}{\boldsymbol{\partial t}} \tag{1}$$

where μ is the magnetic permeability, σ is the electrical conductivity, and $J_e(t)$ is the source current density vector. Once *A* is solved, the magnetic flux density is derived as:

$$B = \nabla \times A \tag{2}$$

Physically, the electromagnetic force generation follows the Lorentz force law. Consequently, the interaction between the magnetic flux density vector (*B*) and the winding current density vector (*J*) induces distributed electromagnetic forces on the conductors. The total electromagnetic force (*F*) acting on the winding volume is theoretically defined as the volume integral of the cross product between *J* and *B:*

$$F = \int_V (J \times B) dV \tag{3}$$

where *F* is the total electromagnetic force vector, *J* is the current density vector, *B* is the leakage magnetic flux density vector and *V* represents the volume of winding conductors.

However, within the numerical framework of this study (Ansys Maxwell), the Principle of Virtual Work is employed to compute these forces with higher stability [1]. Instead of direct integration, the nodal forces are derived by evaluating the variation of the total stored magnetic energy (W) with respect to a virtual displacement (s):

$$F = \frac{dW_{(s,i)}}{ds} = \frac{\partial}{\partial s}\left[\int_V \left(\int_0^H B.H\, dV\right)\right] \quad (4)$$

Where:

- F is the nodal electromagnetic force
- $W_{(s,i)}$ denotes the total stored magnetic energy in the system
- s represents the virtual displacement
- V is the volume of the integration domain
- B and H are the magnetic flux density and magnetic field intensity, respectively.

A critical aspect of the vibration analysis is the frequency characteristic of this force. Assuming a sinusoidal excitation current, and since the stored magnetic energy is proportional to the square of the current ($W \propto B^2 \propto i^2(t)$), the resulting force exhibits a frequency doubling characteristic [1][7]:

$$|F| \propto i^2(t) = I^2[cos(2wt + 2\theta)+1] \quad (5)$$

This derivation reveals a critical characteristic of transformer vibration: the electromagnetic force pulsates at a frequency, double that of the electrical current. Therefore, in the context of a 50 Hz operational environment, the winding structure primarily experiences forced vibrations at a frequency of 100 Hz.

2.2. Mechanical equations

The structural dynamic response of the winding is calculated using the Finite Element Method (FEM). The governing equation of motion for the system is given by [14]:

$$[M]\{\ddot{u}\} + [C]\{\dot{u}\} + [K]\{u\} = \{F\} \quad (6)$$

Where:

- $[M]$,$[C]$and $[K]$denote the global mass, damping, and stiffness matrices, respectively.
- $\{\dot{u}\}, \{\ddot{u}\}$, and $\{\ddot{u}\}$ are the nodal displacement, velocity, and acceleration vectors.
- $\{F\}$ is the electromagnetic load vector derived from the interaction described in (4)

It is explicitly noted that since the winding conductors are made of copper (a diamagnetic material), magnetostrictive effects are negligible. Consequently, the load vector $\{F\}$ originates from the Lorentz forces calculated via the virtual work principle in (4).

Prior to the transient response analysis, a modal analysis is conducted to identify the inherent dynamic characteristics including natural frequencies and mode shapes of the winding structure. It is acknowledged that the actual winding assembly involves nonlinear contact behaviors. However, since the standard modal analysis is fundamentally a linear procedure, these contacts are linearized in this step. The winding is assumed to be in a tightly clamped state under pre-stress, where contacts are treated as bonded to determine the fundamental stiffness matrix $[K]$ Consequently, by neglecting damping and external forces ($[C] = 0, \{F\} = 0$), the general equation (6) reduces to the classical eigenvalue problem:

$$([K] - {\omega_n}^2[M])\{\emptyset_n\} = \{0\} \quad (7)$$

where ω_n represents the natural angular frequency and $\{\emptyset_n\}$denotes the corresponding mode shape vector. The results from this analysis are critical to evaluate the risk of resonance,

particularly checking if any natural mode coincides with the dominant electromagnetic excitation frequency of 100 Hz.

2.3. Analytical Verification Model

To validate the numerical fidelity of the finite element discretization, a mesh verification study is performed using a canonical benchmark problem. In this step, a simplified beam model subject to fixed-fixed (clamped) boundary conditions is analyzed. Based on the Euler-Bernoulli beam theory [14], the theoretical natural frequencies (f_n) for the transverse vibration are governed by:

$$f_n = \frac{{\alpha_n}^2}{2\pi}\sqrt{\frac{E \cdot I}{\rho \cdot A \times L^4}} \tag{8}$$

Where:

- L is the span length of the conductor.
- E is the Young's modulus of the material.
- I is the area moment of inertia of the conductor cross-section.
- ρ and A denote the material density and the cross-sectional area, respectively.
- α_n is the frequency coefficient corresponding to the n^{th} vibration mode.

The results obtained from (8) serve as a benchmark. If the natural frequency calculated by the finite element model aligns closely with this analytical solution, the numerical setup is considered validated for the subsequent complex analysis.

3. SIMULATION ANALYSIS

3.1. Construction of the Three-dimensional Model of the Transformer Core

3.1.1 Geometric Description

This paper presents the construction of a 3D FE model for a 115/23 kV, 40MVA, oil-immersed transformer consisting of a three-phase three-limb core and dual windings. To balance computational efficiency with physical accuracy, distinct geometric models are developed for the electromagnetic and structural domains:

a) Electromagnetic Model

For the magnetic field analysis in Ansys Maxwell, the model focuses solely on the active components: the core and windings, as shown in Fig. 1a. Non-magnetic parts (clamps, insulation) are excluded to reduce mesh complexity without affecting the electromagnetic force calculation.

b) Structural Model

In contrast, the structural model in Ansys Mechanical requires full geometric details to determine the correct stiffness and vibration modes. Therefore, clamping plates, and pressing blocks are fully modeled to represent the actual boundary conditions, as depicted in Fig. 1b.

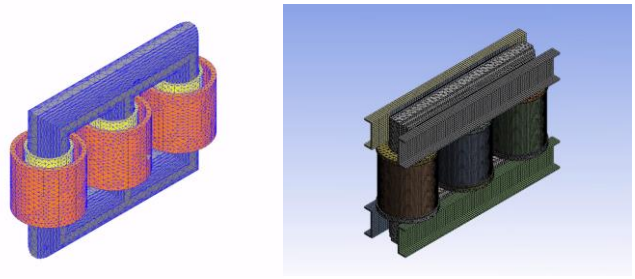

(a) (b)

Fig. 1. 3D geometric models for multiphysics simulation: (a) Electromagnetic model (Ansys Maxwell), (b) Detailed structural model (Ansys Mechanical)

3.1.2. Material Properties

To ensure high simulation fidelity, specific material properties are assigned to each component based on their physical functions in the transformer assembly. The material assignments are defined as follows:

a) Active parts

In the electromagnetic simulation, the magnetic properties of the iron core are characterized by a nonlinear B-H curve to account for saturation effects, while hysteresis losses are considered negligible. Regarding the windings, a "stranded conductor" model is adopted. This formulation assumes that the coils consist of numerous thin turns with diameters significantly smaller than the skin depth at the operating frequency. Consequently, the eddy current distribution within individual wire cross-sections is disregarded.

b) Structural Parts

The clamping frame uses structural steel to support the core and windings. To apply pressure on the windings, birch wood blocks are used. Additionally, a pressboard layer is placed between the steel clamps and the core. This layer acts as a cushion to prevent direct metal contact and reduce vibration stress. The mechanical properties for these materials are listed in Table I.

Table 1. Material properties

Component	Material	Density (kg/m^3)	Young's Modulus (GPa)	Poisson's Ratio
Core	Silicon Steel	7895	207	0.295
Windings	Copper	8942	120	0.345
Clamps	Structural Steel	7850	200	0.3
Pressing Block	Birch Wood	686.4	15.17	0.3742
Insulation Layer	Paper (cellulose based)	897.2	2.828	0.3674

3.2. Simulation Workflow

The overall research methodology is systematized in the flowchart presented in Fig. 2. The process is structured into two sequential phases to ensure the reliability of the numerical results:

3.2.1. Mesh Verification Strategy

Prior to the complex multiphysics simulation, a preliminary study is conducted to determine the optimal mesh size. A simplified FEM Beam model is constructed and compared

against the Analytical Beam Theory. The discretization quality is considered acceptable only when the relative error of the natural frequency between the numerical and analytical results satisfies the convergence criterion (Error < 5%). The verified mesh parameters are then extracted for the main simulation.

3.2.2. Multiphysics Coupling

Once the mesh parameters are verified, they are applied to the 40 MVA transformer simulation in this phase, which employs a one-way electromagnetic-structural coupling scheme:

a) Electromagnetic Field

The process begins in Ansys Maxwell, where the transient magnetic field is solved to calculate the volumetric Electromagnetic Forces.

b) Structural Field

Simultaneously, the detailed structural model is set up in Ansys Mechanical using the verified mesh extracted from the previous phase. The volumetric Lorentz forces, calculated via the virtual work principle in the electromagnetic domain, are exported as nodal force vectors. These forces are then imported into the structural model using a volumetric spatial mapping algorithm to ensure accurate load transfer onto the structural nodes.

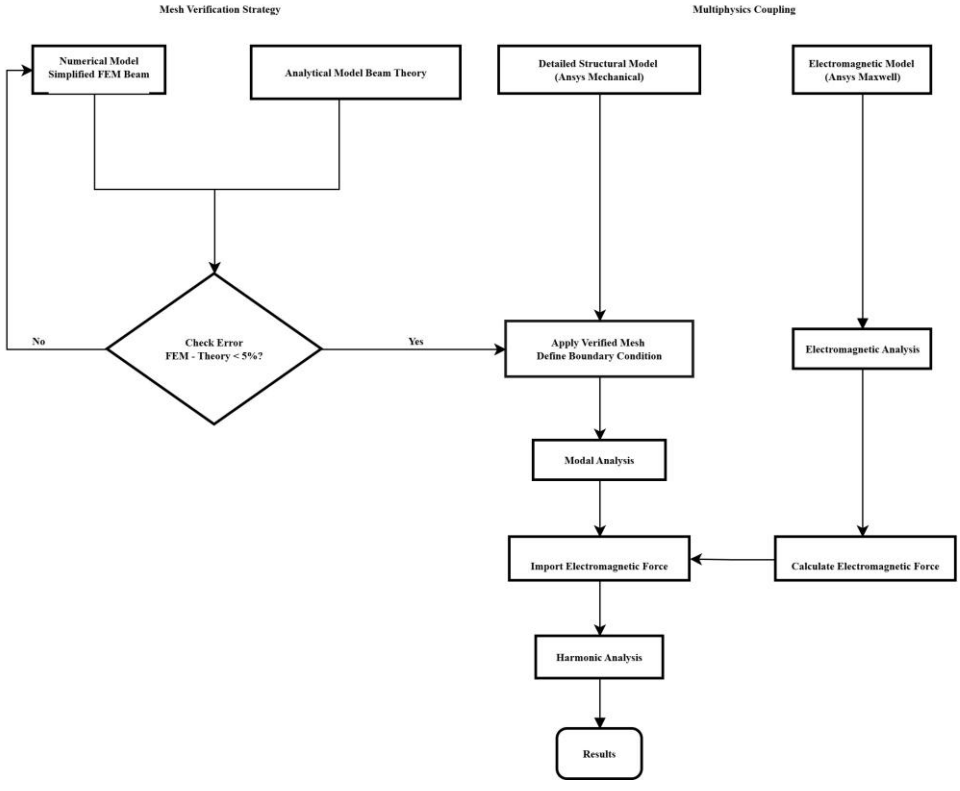

Fig. 2. Flowchart of the proposed simulation strategy: Mesh verification and Multiphysics coupling

3.3. Simulation Result Analysis

3.3.1. Verification Study

In this section, a canonical fixed-fixed (clamped) beam problem is analyzed to verify the reliability of the finite element discretization strategy. Instead of modeling the complex winding geometry directly, a simplified generic beam is used as a benchmark case. The geometric dimensions of this benchmark model are defined as follows: length L= 1 m, width b = 0.05 m, and thickness h = 0.02 m. These specific dimensions were selected to approximate the typical aspect ratio of the actual winding conductors used in the 40 MVA transformer, providing a structurally representative baseline. Although the actual winding is a composite structure of copper and paper insulation, the copper conductors dictate the dominant structural stiffness and mass. Therefore, verifying the mesh parameters on a homogenous beam model serves to isolate and validate the numerical finite element discretization against an exact analytical solution before applying these settings to the complex 3D composite assembly. Furthermore, while altering these initial dimensions would naturally shift the theoretical natural frequencies, the fundamental mesh convergence trend and the relative error margin remain consistent within the linear elastic regime.

The theoretical natural frequencies are calculated using (8), with the mode shape coefficients (α_n) for a clamped-clamped beam adopted from [14]. Based on this extensive testing, a mesh size of 0.01 mm was selected as the optimal parameter.

Table II presents the comparison between the analytical and numerical results for the first six vibration modes. It is important to note that the finite element simulation captures multiple degrees of freedom, resulting in a combination of vibration modes along different axes; specifically, Modes 1, 3, 4, and 6 correspond to transverse bending along the weaker axis, while Modes 2 and 5 represent lateral bending along the stronger axis.

The relative error between the simulation and the analytical solution remains consistently low across all identified modes (maximum deviation < 3.5%), confirming that the selected mesh density is sufficiently refined to accurately predict the structural response of the transformer windings.

Table 2. Comparison of analytical and simulation results

Mode	Analytical Frequencies (Hz)	Simulation Frequencies (Hz)	Error (%)
1	74.84	75.43	0.78
2	187.11	184.78	1.26
3	206.29	207.27	0.47
4	404.47	404.66	0.05
5	515.74	498.58	3.44
6	668.55	665.49	0.46

To extend this verification from the fundamental beam to the full-scale structure, a brief mesh sensitivity check was subsequently performed on the complete 3D winding-clamp assembly. The results confirmed that further mesh refinement beyond the selected density did not produce noticeable variations in the natural frequency near 100 Hz (Mode 3) or the peak displacement values, thus ensuring the computational stability of the model.

Table 3. Mesh sensitivity results for full transformer model

Mesh Case	Number of Elements	Natural Frequency f3 (Hz)	Peak Displacement (×10−6 m)
Coarse	284,512	100.24	4.98
Medium (Selected)	642,185	99.158	4.86
Fine	1,145,630	99.102	4.81

3.3.2. Electromagnetic Field Analysis

The electromagnetic transient analysis is driven by a sinusoidal three-phase voltage source excitation. To capture the full dynamic behavior, the simulation duration is set to 400 ms, corresponding to 20 electrical cycles at 50 Hz. The time domain is discretized into 800 equal steps, yielding a time step of 0.5 ms.

a) Magnetic Flux Density

Fig. 3 illustrates the magnetic flux density distribution in the core at the time instance of peak current. As observed, the magnetic flux is well-confined within the core, with a maximum flux density of approximately 1.86 T, which is below the saturation limit of silicon steel material. The leakage flux fringes into the winding domain, interacting with the load current to generate electromagnetic forces.

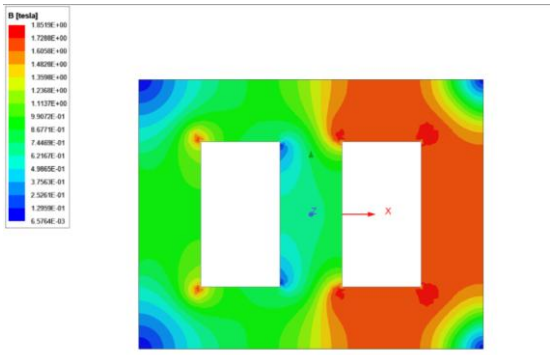

Fig. 3. Magnetic flux density distribution in the transformer core at rated load at 330ms.

b) Electromagnetic Force Distribution

The electromagnetic forces acting on the windings are computed using the Principle of Virtual Work, consistent with the theoretical framework outlined in Section II.

After 225 ms fluctuations, the electromagnetic field reaches a steady state. Fig. 4 presents the time-domain evolution of the electromagnetic forces acting on the Phase A High Voltage (HVA) with x, y and z directions. These results are presented as a representative case for the other windings.

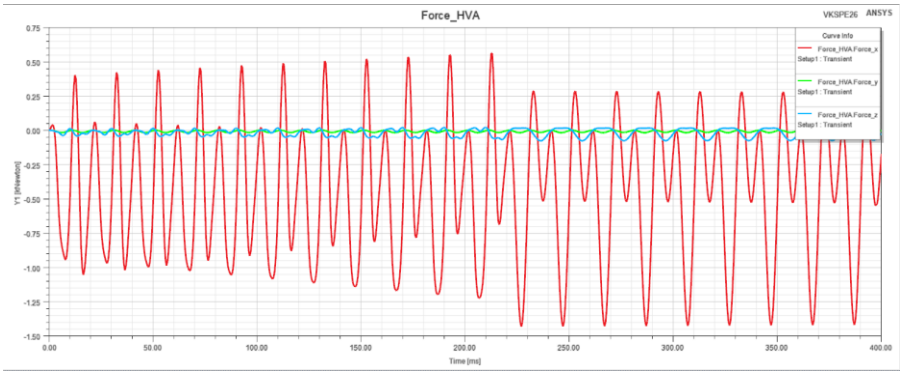

Fig. 4. Electromagnetic force of high voltage windings phase A

As demonstrated in Fig. 4, the electromagnetic forces exhibit a periodic variation with time. The observed period is 10 ms, which corresponds to half the period of the sinusoidal excitation current. The force waveform is non-sinusoidal, indicating the presence of numerous harmonic components. The simulation results indicate peak forces of F_x is 0.56

kN, F_y = 0.018 kN and F_z = 0.077 kN. Consequently, the force in the x-direction dominates over the y- and z-directions.

3.3.3. Magnetic-Structure Coupling Field Analysis

a) Modal Analysis

Modal analysis is performed to determine the inherent dynamic characteristics of the model structure. This step is crucial to identify potential resonance risks where the natural frequencies (f_n) might coincide with the electromagnetic excitation frequency of 100 Hz. From the simulation results, the first six natural frequencies of the model are identified as follows:

f_1= 55.291 Hz, f_2= 78.283 Hz, f_3= 99.158 Hz, f_4= 158.01 Hz, f_5 = 182.23 Hz, f_6 = 214.92 Hz.

Based on the modal analysis, Mode 3 at 99.158 Hz is identified as the natural frequency closest to the excitation source. This extremely narrow amplitude indicates a significant risk of resonance under steady-state operation.

b) Harmonic Response Analysis

To quantify the vibration risks and validate the linear elastic assumption stated in the methodology, the harmonic response under steady-state operation is analyzed. To account for the energy dissipation mechanisms within the transformer, such as oil viscosity and insulation friction, a constant damping ratio equal 0.03 is applied [1][14]. It should be noted that this damping value represents optimal conditions with healthy transformer oil and intact paper insulation. Over long-term operation, practical factors such as oil aging, thermal degradation, and moisture ingress can reduce the system's damping capacity. Under such degraded conditions, the winding structure may become more sensitive to dynamic loads, potentially amplifying the resonance amplitude beyond the baseline calculations.

Fig. 5 illustrates the displacement amplitude and phase angle of the transformer structure across the frequency range of 10-200 Hz. A significant resonance peak is observed specifically at the excitation frequency of 100 Hz, corresponding to a maximum displacement amplitude of 4.86 x 10^{-6} m.

This amplification is attributed to the proximity between the electromagnetic excitation frequency (100 Hz) and the structure's third natural frequency (Mode 3), which was determined to be 99.158 Hz from the modal analysis. The negligible frequency deviation indicates a critical resonance condition.

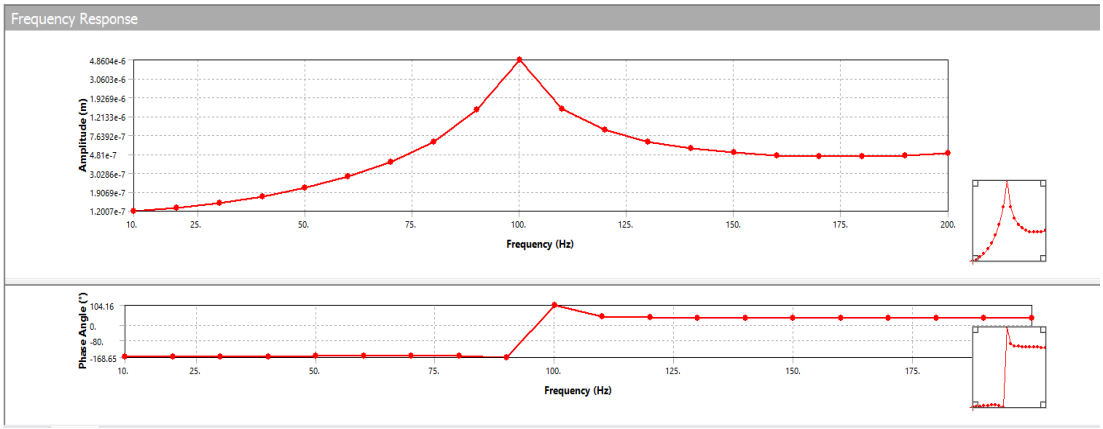

Fig. 5. The displacement amplitude and phase angle of the transformer structure across the frequency range of 10-200 Hz

As illustrated in Figs. 6 and Fig. 7, the deformation profile along the axial height (Z-direction) of the high voltage winding exhibits a smooth, arch-shaped curve. Due to the mechanical

constraints imposed by the top and bottom clamping structures, the displacement at both ends is negligible, while the maximum deformation occurs at the mid-height of the winding.

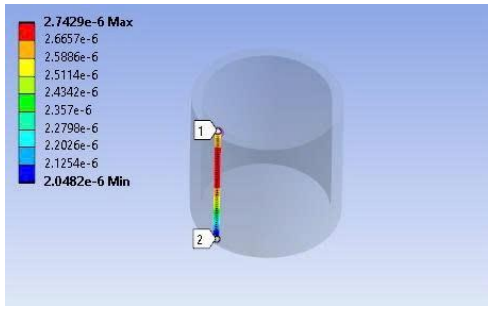

Fig. 6. Radial deformation contour plot and definition of the axial path (along the Z-axis) used for displacement evaluation

This winding expands outward with a peak displacement of to 2.74 x 10^{-6} m, indicating that the electromagnetic forces act predominantly in the radial outward direction. A similar deformation pattern is observed in the low voltage winding; however, in this case, the winding is compressed inward toward the core. The maximum displacement reaches 2.97 x 10^{-6} m, slightly exceeding that of the HV winding. This difference can be attributed to the proximity of the LV winding to the magnetic core, where stronger inward-directed electromagnetic forces result in a marginally larger bending deformation.

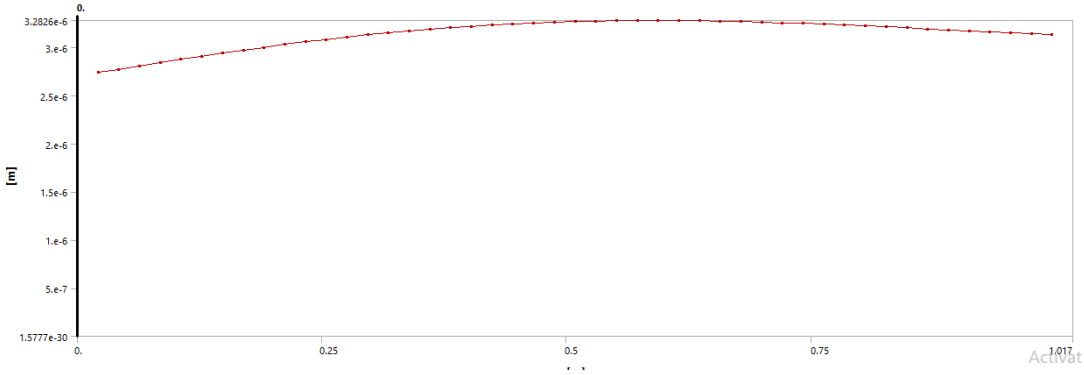

Fig. 7. Graph showing the radial deformation distribution along the HV winding height

To synthesize the dynamic behavior of the transformer, Table IV summarizes the critical modal frequencies and the peak radial vibration results for both the High Voltage (HV) and Low Voltage (LV) windings under the 100 Hz electromagnetic excitation.

Table 4. Summary of vibration characteristics

Parameter	High Voltage (HV) Winding	Low Voltage (LV) Winding
Critical Natural Frequency (Mode 3)	99.158 Hz	99.158 Hz
Excitation Frequency	100 Hz	100 Hz
Peak Radial Displacement	2.74 x 10^-6 m	2.97 x 10^-6 m

4. CONCLUSION

This paper successfully established a rigorous multiphysics simulation framework to analyze the electromagnetic vibration of a 40 MVA power transformer winding. By integrating analytical verification with Finite Element Analysis (FEA), the study bridges the gap between

theoretical fundamentals and complex numerical modeling. The key findings are summarized as follows:

Validation of Numerical Accuracy: The proposed mesh verification strategy, benchmarked against the analytical Euler-Bernoulli beam theory, achieved a high degree of convergence with a relative error of less than 3.5% for the first six vibration modes. This confirms that the finite element discretization is physically accurate, mitigating the uncertainty often encountered in FEA.

The modal analysis revealed that the winding's third natural frequency (f_3= 99.158 Hz) is critically close to the dominant electromagnetic excitation frequency of 100 Hz. The harmonic response analysis confirmed a distinct resonance peak at 100 Hz, accompanied by a sudden phase shift characteristic of resonance. At this resonance point, the maximum radial displacement of the entire winding assembly reached 4.86 x 10^{-6} m. This global maximum value encompasses the individual deformation peaks observed in the high voltage and low voltage windings 2.74 x 10^{-6} m and 2.97 x 10^{-6} m, respectively. This result indicates that while structural damping prevents infinite displacement, the resonance condition significantly amplifies the vibration amplitudes compared to non-resonant frequencies.

REFERENCES

[1] S. V. Kulkarni and S. A. Khaparde, *Transformer Engineering: Design, Technology, and Diagnostics*, 2nd ed. Boca Raton, FL, USA: CRC Press, 2012. Available: https://electricalconnects.com/frontend/images/free_items/transformer-engineering-design-technology-and-diagnostics-2nd-edition-by-s-v-kulkarni-and-s-a-khaparde.pdf

[2] L. Ying, D. Wang, J. Wang, G. Wang, X. Wu, and J. Liu, "Power transformer spatial acoustic radiation characteristics analysis under multiple operating conditions," *Energies (Basel).*, vol. 11, no. 1, Jan. 2018, doi: https://doi.org/10.3390/en11010074.

[3] N. Yu, B. An, Q. Yu, M. Xia, Y. Liu, and Q. Li, "Research on Vibration of Transformer Core Based on Finite Element Method," in *International Conference on Advanced Electrical Equipment and Reliable Operation, AEERO 2021*, Institute of Electrical and Electronics Engineers Inc., 2021. doi: https://doi.org/10.1109/AEERO52475.2021.9708398.

[4] Z. Chen, Q. Zhou, G. Ding, X. W. Wu, J. Wu, and Y. Zhang, "Influence of Magnetic State Variation on Transformer Core Vibration Characteristics and Its Measurement," *IEEE Trans. Instrum. Meas.*, vol. 71, 2022, doi: https://doi.org/10.1109/TIM.2022.3186377.

[5] Do Chi Phi, Doan Thanh Bao, Phung Anh Tuan, Le Van Doanh, "A study of the effect of magnetostriction on the deformation of the steel core in amorphous transformers", *The University of Danang - Journal of Science and Technology*, vol. 11, no. 96.2, Nov. 2015, pp. 130-135, https://jst-ud.vn/jst-ud/article/view/2859

[6] H. Jingzhu, L. Dichen, L. Qingfen, Y. Yang, and L. Shanshan, "Electromagnetic vibration noise analysis of transformer windings and core," *IET Electr. Power Appl.*, vol. 10, no. 4, pp. 251–257, Apr. 2016, doi: https://doi.org/10.1049/iet-epa.2015.0309.

[7] L. Naranpanawe and C. Ekanayake, *Finite element modelling of a transformer winding for vibration analysis*. Brisbane, QLD, Australia: 2016 Australasian Universities Power Engineering Conference (AUPEC), 2016, doi: https://doi.org/10.1109/AUPEC.2016.7749344.

[8] P. Witczak and M. Swiatkowski, "Transmission of Vibrations from Windings to Tank in High Power Transformers," *Energies (Basel).*, vol. 16, no. 6, Mar. 2023, doi: https://doi.org/10.3390/en16062886.

[9] B. García, J. C. Burgos, and Á. M. Alonso, "Transformer tank vibration modeling as a method of detecting winding deformations - Part I: Theoretical foundation," *IEEE Transactions on Power Delivery*, vol. 21, no. 1, pp. 157–163, Jan. 2006, doi: https://doi.org/10.1109/TPWRD.2005.852280.

[10] Z. Li *et al.*, "Research on electromagnetic vibration and noise of transformer under short circuit conditions," *AIP Adv.*, vol. 15, no. 3, Mar. 2025, doi: https://doi.org/10.1063/5.0248074.

[11] L. He, Y. Zhu, G. Liu, and C. Cao, "Simulation analysis and experiment research of transformer vibration based on electric–magnetic–mechanic coupling," *Energies (Basel).*, vol. 18, no. 9, May 2025, doi: https://doi.org/10.3390/en18092238.

[12] L. Hui, Z. Bin, C. Jiangbo, C. Chen, and W. Yang, "Simulation and Test on Vibration Characteristics of Power Transformer Windings," in *Proceedings of the 2015 International Symposium on Computers & Informatics (ISCI 2015),* Atlantis Press, Jan. 2015, pp. 1259–1267. doi: https://doi.org/10.2991/isci-15.2015.167.

[13] D. Marcsa, "Noise and vibration analysis of a distribution transformer," *Przeglad Elektrotechniczny*, vol. 95, no. 12, pp. 172–175, 2019, doi: https://doi.org/10.15199/48.2019.12.38.

[14] S. S. Rao, *Mechanical vibrations*. Prentice Hall, 2011. Available: https://archive.org/details/mechanicalvibrat0000raos_a3e9